THE JOURNAL OF PHYSICAL CHEMISTRY B

Article

pubs.acs.org/JPCB

Hydration Shell Parameters of Aqueous Alcohols: THz Excess Absorption and Packing Density

V. Matvejev,*[,†] M. Zizi,[‡] and J. Stiens[§,†]

[†]Laboratory of Micro- and Photonelectronics LAMI-ETRO, Vrije Universiteit Brussel, Pleinlaan 2, B-1050 Brussels, Belgium

[‡]Department of Physiology FYSP, Vrije Universiteit Brussel, Laarbeeklaan 101B, B-1090 Brussels, Belgium

[§]Unit SSET, Department HIM, Group RFCDM, IMEC, Kapeldreef 75, B-3001 Leuven, Belgium

ABSTRACT: Solvation in water requires minimizing the perturbations in its hydrogen bonded network. Hence solutes distort water molecular motions in a surrounding domain, forming a molecule-specific hydration shell. The properties of those hydration shells impact the structure and function of the solubilized molecules, both at the single molecule and at higher order levels. The size of the hydration shell and the picoseconds time-scale water dynamics retardation are revealed by terahertz (THz) absorption coefficient measurements. Room-temperature absorption coefficient at $f = 0.28$ [THz] is measured as a function of alcohol concentration in aqueous methanol, ethanol, 1,2-propanol, and 1-butanol solutions. Highly diluted alcohol measurements and enhanced overall measurement accuracy are achieved with a THz absorption measurement technique of nL-volume liquids in a capillary tube. In the absorption analysis, bulk and interfacial molecular domains of water and alcohol are considered. THz ideal and excess absorption coefficients are defined in accordance with thermodynamics mixing formulations. The parameter extraction method is developed based on a THz excess absorption model and hydrated solute molecule packing density representation. First, the hydration shell size is deduced from the hydrated solute packing densities at two specific THz excess absorption nonlinearity points: at infinite alcohol dilution (IAD) and at the THz excess absorption extremum (EAE). Consequently, interfacial water and alcohol molecular domain absorptions are deduced from the THz excess absorption model. The hydration shell sizes obtained at the THz excess absorption extremum are in excellent agreement with other reports. The hydration shells of methanol, ethanol, 1- and 2-propanol consist of 13.97, 22.94, 22.99, and 31.10 water molecules, respectively. The hydration shell water absorption is on average 0.774 ± 0.028 times the bulk water absorption. The hydration shell parameters might shed light on hydration dynamics of biomolecules.

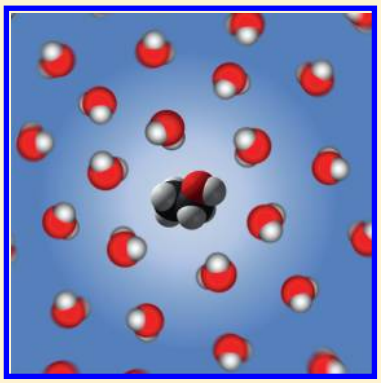

INTRODUCTION

In recent years, there has been an increasing interest in the bidirectional interactions between biomolecules and "biological" water, i.e., the hydration shell. A recent study[1] shows the coupling of the hydration water with the active enzymatic site of a protease during peptide hydrolysis. Protein conformational changes are coupled with hydration shell variations,[2,3] and the hydration shells around amino acids are determined by the hydrophilic[4] and hydrophobic[5] nature of their interfacing surfaces. All those hydration shell fluctuations are detectable by THz ($f > 0.1$ [THz][6,7]) absorption measurements. The usage of THz waves is advantageous since it involves direct water probing on the picosecond time scale, which corresponds to the reorientation time of the water molecule. Therefore, THz absorption coefficient measurements enable label-free, real-time biosensing via hydration shell observations.

The intermolecular interaction differences of solvent−solute relative to solute−solute and solvent−solvent causes spatial and dynamic[8,9] perturbations of both solvent and solute molecules near the interface. This interfacial layer—either hydration or solvation shell—is defined as a layer of molecules with perturbed spatial and dynamic properties with respect to the same molecules in bulk. The perturbation strength and its spatial extent depend on the solute molecules' hydrophobic and hydrophilic (charged and noncharged) surfaces properties, their distributions and three-dimensional shape.[10] Hydration shell water absorbs differently than bulk water.[11] Static structure enhancements around solute molecules are not observed,[12] therefore the different hydration shells can overlap. All these effects contribute to the nonlinearity in the THz absorption coefficient versus solute concentration in aqueous solutions.

It would thus be of interest to learn how to extract the hydration shell properties from the THz absorption coefficient dependency on solute concentration. The research group of M. Havenith reported THz absorption coefficient measurements on highly hydrated biomolecules.[3,8,13−15] The hydration shell analysis is done with the three component (bulk water, hydration shell water and solute) THz absorption coefficient model[8] and, is focused on the highly diluted concentration range. At infinite dilution, solute molecules and their hydration shells are represented by uniformly distributed individual spheres in the bulk water. With increasing solute concentration

Received: June 1, 2012
Revised: November 15, 2012
Published: November 15, 2012

the average distance between spheres decreases and then the spheres begin to overlap. It is assumed that water molecules belonging to multiple hydration shells exhibit the same dynamics as those belonging to a single hydration shell. The overlap of the hydration shells results in deviation from linearity of the absorption coefficient dependency on solute concentration at the infinite dilution transition concentration. Therefore, the hydration shell size is extracted from the solute concentration at this deviation point. However, the measurements at infinite dilution are prone to noise leading to larger extraction errors. Moreover, the concentration range with linear absorption dependency is questionable. Hence, other specific solute concentrations points in the THz absorption coefficient dependency must be found to obtain more reliable hydration shell estimations.

The primary focus of this paper is a hydration shell parameter extraction methodology from the dependency of the THz absorption coefficient on solute concentration. The methodology is demonstrated with aqueous lower alcohol solutions of methanol, ethanol, 1,2-propanol, and 1-butanol. On the basis of discussed hydration/solvation shell properties following *assumptions* are taken during the analysis: (1) four-component total absorption model—bulk water, hydration shell water, solvation shell alcohol, and bulk alcohol; (2) concentration independent component THz absorption; (3) concentration dependent component volume fraction; (4) spherical molecule and its shell; (5) overlap of the hydration/solvation shells; (6) hydration/solvation shell properties are uniform, i.e., not dependent on the distance to interfaces; (7) hydration/solvation shell material density is the same as in bulk; (8) negligibly small self-association. The validity of the assumptions is discussed. In accordance with thermodynamics the definition of an ideal mixing THz absorption coefficient is given. Then the THz excess absorption coefficient expression is derived. The THz excess absorption coefficient is dependent on hydration shell size and hydration water THz absorption. In order to separate the hydration shell absorption coefficient and size, first, a hydration shell size extraction method is developed. This method is based on specific nonlinearity points of the THz excess absorption coefficient and the hydration shell geometrical packing considerations. Hydration shell packing at infinite alcohol dilution and THz excess absorption coefficient maxima are considered. The hydration shell water and solvation shell alcohol absorption coefficients are then derived knowing the hydration shell size.

EXPERIMENTAL METHODS

A highly sensitive and extremely accurate integrated sensor configuration, reported in,[16] is used for THz absorption measurements of aqueous alcohol solutions. The sensor configuration uses an integrated, low-loss waveguide[17] and a commercially available capillary tube with an internal diameter of 320 [μm]. The capillary tube passes through the center of the broad-wall of the waveguide, penetrating the waveguide perpendicularly to the wave propagation direction and in parallel to the electric field vector, allowing efficient interaction between the liquid and the THz electromagnetic wave.

The sensors' scattering parameters in WR-3.4 band (f = 226−336 [GHz]) are measured with an *AB Millimeter* Millimeter-wave Vector Network Analyzer. The absorption is calculated from the measured transmission parameter $T = 20 \times \log(I/I_0)$ using formula $I = I_0 e^{-\alpha d}$, where d is the equivalent propagation distance inside the capillary tube. By normalizing the THz absorption coefficient of a solution to the THz absorption coefficient of pure water, the distance factor is canceled. For any of the aqueous alcohol solutions measured, the sensor transmission coefficient shows a typical trend to reduce with the frequency. The decrease is strongly pronounced for water and much less for alcohols. This corresponds to a liquid absorption increase with frequency. The analysis is done on measurements at f = 0.28 [THz] since measured transmission parameters show only a monotonous frequency dependence.

The intensity of the EM-wave incident on the liquid, I_0, depends on the reflection on the capillary tube air-wall and wall-liquid interfaces, and therefore depends on the liquid. For technical reasons the reflection signal could not be measured and was neglected during the absorption coefficient derivation. Nevertheless the error introduced is small, since the reflection change for such a sensor configuration is very limited: finite element method simulations show that at f = 0.28 [THz] the reflection changes from −14.0 [dB] for water to −12.8 [dB] for methanol (3% of I_0). Any of the internal reflections are absorbed within the liquids.

Water−alcohol solutions are prepared with 18 [MW] Milli-Q water and analytical grade (99,8% pure) alcohols. The molar fractions are mixed proportionally according to molecular weights using a laboratory balance with 0.1 [mg] precision. The mixture is prepared in a 5 [mL] boiling tube filled almost to the top. The tubes with prepared mixtures are covered with parafilm to prevent degassing, and are left to cool down to room-temperature after mixing (exothermic reaction). Before each water−alcohol THz absorption measurement, syringe and capillary tube are flushed with a water−alcohol mixture of the same concentration.

RESULTS

The normalized absorption of aqueous alcohol solutions are plotted against the alcohol molar fraction in Figure 1. The smallest alcohol to water molar fraction measured is $x_A = 4 \times 10^{-4}$ [mol/mol] for ethanol (equivalent mass concentration ρ_A = 1.02 [g/L]). The aqueous alcohol absorption exhibits a nonlinear dependence on alcohol concentration. The absorption gradually decreases with the increase in alcohol concentration, more strongly at low concentrations first and then in a less pronounced manner at higher concentrations. The measured absorption behavior for the aqueous ethanol compares well to the one reported in[18] at f = 0.5 [THz]. The nonlinearity increases with increasing alcohol size, or the length of the hydrophobic carbohydrate chain. Normal and isomeric propanol alcohols do not have the same THz absorption over concentration dependency, even though their bulk absorption coefficients are very close. Aqueous 1-butanol measurements in the concentration range (x_A = 0.03−0.5 [mol/mol]) are not included, because 1-butanol is not miscible at these concentrations. The measured normalized bulk alcohol absorptions are consistent with.[19,20]

THz Excess Absorption Coefficient. Starting from Maxwell equations, the EM-wave power loss in a dielectric medium is related to the absorption coefficient by the following relation:[22]

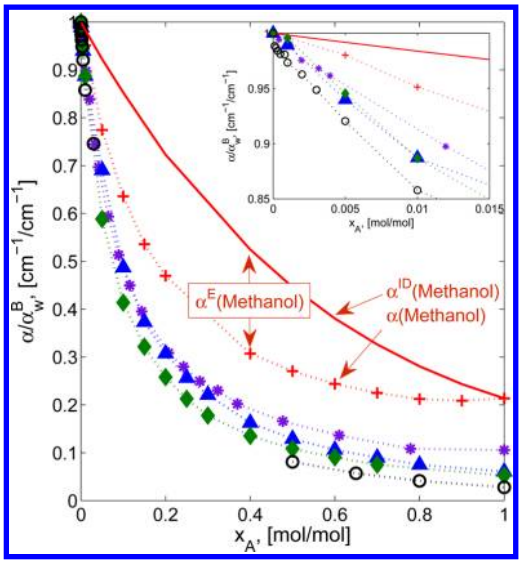

Figure 1. Normalized aqueous alcohol (f = 0.28 [THz]) absorption coefficient dependency on alcohol concentration for lower alcohols: methanol (red +), ethanol (purple ∗), 1-propanol (blue △), 2-propanol (green ◇), 1-butanol (○). The dotted lines are guide to the eye. Aqueous methanol excess absorption and ideal mixture (solid line) absorption demonstration. Inset: detailed view on absorption behavior of diluted alcohol solutions.

$$P_l = \frac{1}{\sqrt{\varepsilon_0\mu_0}}\int_v \alpha|\vec{E}|\,dV = \frac{1}{\sqrt{\varepsilon_0\mu_0}}\left(\int_{v_1}\alpha_1|\vec{E}|\,dV + \int_{v_2}\alpha_2|\vec{E}|\,dV + \ldots + \int_{v_i}\alpha_i|\vec{E}|\,dV\right) \quad (1)$$

The equation is reformulated according to Bruggemann is effective medium approximation: a dielectric medium, consisting of uniformly distributed subdomains (v_i, α_i), orders of magnitude smaller than the EM-wave wavelength, is treated as a uniform medium with an effective dielectric properties (v, α). For a volume with uniform E-field distribution eq 1 becomes:

$$\alpha V_{\text{Total}} = \alpha_1 V_1 + \alpha_2 V_2 + \ldots + \alpha_i V_i \quad (2)$$

The total THz absorption coefficient, α, in a distributed solution is a weighted sum of the solution constituents THz absorption coefficients, α_i, with volume fractions as a weighting factors $\Phi_i = V_i/V_{Total}$:

$$\alpha = \sum_i \alpha_i\Phi_i = \sum_i \overline{V}_i\alpha_i c_i \quad (3)$$

The second equality in eq 3 shows the concentration c_i dependence of the total absorption, in accordance with Beer–Lambert law.

The volume fractions of alcohol $\Phi_A(x_A)$ and water $\Phi_W(x_A)$ are derived by means of their concentration dependent partial molar volumes $\overline{V}_A(x_A)$, $\overline{V}_W(x_A)$, whereby $\Phi_A(x_A) = \overline{V}_A(x_A)\cdot x_A/(\overline{V}_A(x_A)\cdot x_A + \overline{V}_W(x_A)\cdot x_W)$ and $\Phi_W(x_A) = 1 - \Phi_A(x_A)$. The expression for the partial molar volumes read as follows:

$$\overline{V}_i(x_i) = V^E(x_i) + V_i^\circ + (1 - x_i)\left(\frac{\partial V^E}{\partial x_i}\right)_{p,T}\Bigg|_{x_i} \quad (4)$$

where V_i° is pure water or alcohol molar volume, V^E water–alcohol mixing excess molar volume found in.[23,24] Note that, partial molar volume (expressed in [cm^3/mol]) includes the density changes during the water–alcohol mixing.

When water and alcohol are mixed together, the THz absorption of the resulting mixture is different from the *ideal mixture THz absorption*, α^{ID}, behavior which reads as

$$\alpha^{ID}(x_A) = \alpha_W^B\Phi_W(x_A) + \alpha_A^B\Phi_A(x_A) \quad (5)$$

where water and alcohol do not interact, exhibiting the same absorption when unmixed. The α^{ID} has a linear dependency on alcohol volume fraction in the solution, but when plotted versus the alcohol molar fraction it becomes nonlinear (e.g., aqueous methanol α^{ID} is shown in Figure 1).

At any given composition, molecules constituting a mixture may (according to the assumption) exhibit bulk- and interfacial-like properties. Hence, four distinct domains are considered in a binary water–alcohol mixture see Table 1. Consequently, the generic four-component THz absorption model reads as

$$\alpha(x_A) = \alpha_W^B\Phi_W^B(x_A) + \alpha_W^H\Phi_W^H(x_A) + \alpha_A^S\Phi_A^S(x_A) + \alpha_A^B\Phi_A^B(x_A) \quad (6)$$

Table 1. Domains Contributing to THz Absorption in the Four-Component Model and Their Relations

	absorption		volume fraction	
molecule domain	α_i	definitions	Φ_i	relations
bulk water	α_W^B	$\Delta\alpha_W^{HB} = \alpha_W^H - \alpha_W^B$	Φ_W^B	$\Phi_W^B + \Phi_W^H = \Phi_W$
hydration shell water	α_W^H		Φ_W^H	
solvation shell alcohol	α_A^S	$\Delta\alpha_A^{SB} = \alpha_A^S - \alpha_A^B$	Φ_A^S	$\Phi_W + \Phi_A = 1$
bulk alcohol	α_A^B		Φ_A^B	$\Phi_A^B + \Phi_A^S = \Phi_A$

The departure from the ideal mixing case (e.g., for aqueous methanol Figure 1) is expressed by the *THz excess absorption coefficient*, α^E. It reflects the level of the intermolecular interactions in the solution resulting in the creation of hydration and solvation shells. In analogy to the thermodynamic excess quantities, the THz excess absorption coefficient is defined as

$$\alpha^E \equiv \alpha - \alpha^{ID} \quad (7)$$

The THz excess absorption is expressed using eq 5, eq 6 and Table 1 equations as:

$$\alpha^E(x_A) = \Delta\alpha_W^{HB}\Phi_W^H(x_A) + \Delta\alpha_A^{SB}\Phi_A^S(x_A) \quad (8)$$

Equation 8 is valid over the whole concentration range.

Using the estimated volume fractions, eqs 5 and 7 and THz absorption measurements in Figure 1, the THz excess absorption α^E is calculated and shown in Figure 2. The 3-term function $f_{\text{INT}}(x_A)$:

$$f_{\text{INT}}(x_A) = x_A\sum_{i=1}^{3} a_i e^{-b_i x_A} \quad (9)$$

is used to interpolate and smooth the measurement data over the whole concentration range. The fitting results in a very small RMS error: 4.4×10^{-3}, 2.6×10^{-3}, 12.7×10^{-3}, and 4.2×10^{-3} for methanol, ethanol, and 1,2-propanol, respectively.

The THz excess absorption in a binary solution is a combination of two effects: existence of hydration/solvation shells (Φ_W^H, Φ_A^S) and THz absorption difference ($\Delta\alpha_W^{HB}$, $\Delta\alpha_A^{SB}$) compared to bulk domains. The volume fractions of molecules in hydration and solvation shells change with solution

dx.doi.org/10.1021/jp305356d | J. Phys. Chem. B 2012, 116, 14071–14077

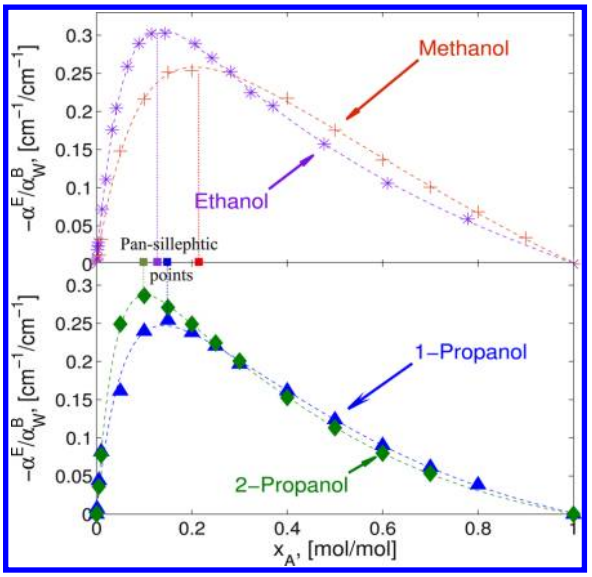

Figure 2. The normalized THz excess absorption coefficient (f = 0.28 [THz]) of aqueous alcohol mixtures and their pansyllephtic points: (a) methanol (red +), ethanol (purple ∗); (b) 1-propanol (blue △), 2-propanol (green ◇). The dotted lines represent fitting results.

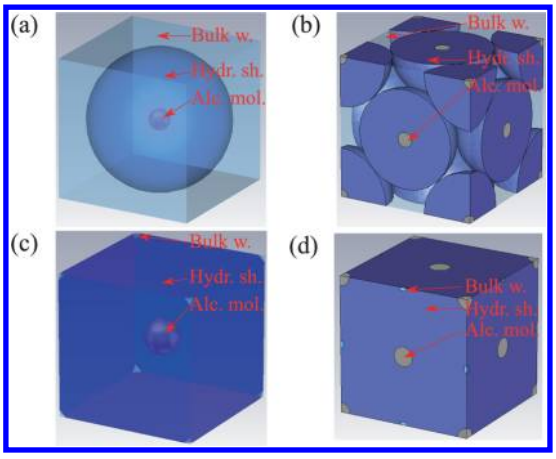

Figure 3. Hydration shell packing. IAD is represented by packed nonoverlapping sphere lattices: (a) simple cubic ($\eta_1 = (\pi/6) \approx 0.52$) and (b) face-centered cubic ($\eta_1 = (\pi/(3\sqrt{2})) \approx 0.74$) unit cells. EAE is represented by packed overlapping sphere lattices: (c) simple cubic ($\eta_2 = ((\pi\sqrt{6})/2) \approx 2.72$) and (d) face-centered cubic ($\eta_2 = ((2\pi)/3) \approx 2.09$) unit cells.

composition – $[\Phi_W^H, \Phi_A^S] = f(x_A)$, while the THz absorption of mixture constituents are assumed to remain constant – α_i = const. Hydration shell size and THz absorption need to be estimated separately. This is achieved using Figure 2, eq 8 and the methodology described below.

Hydration Shell Size Extraction. In order to dissect in eq 8 the hydration shell size and THz absorption coefficient, some specific features in the concentration-dependence of the THz excess absorption coefficient of Figure 2 are exploited. Here, hydration shell size is expressed in average number of water molecules in the hydration shell of a single solute molecule, N_H. The N_H is estimated using the geometrical representations of hydration shell overlap at two specific alcohol concentrations: at infinite alcohol dilution (IAD) and at the THz excess absorption extremum (EAE).

At *infinite alcohol dilution* (IAD), alcohol molecules in the solution do not influence one another. Each alcohol molecule with its hydration shell can be represented as an individual sphere. The domain inside the spheres comprises the alcohol molecule and the hydration shell water molecules; outside the sphere is bulk water. In this range, the THz excess absorption exhibits a linear behavior versus alcohol concentration. As the alcohol concentration increases, the number of spheres increases and the amount of bulk water reduces. At a specific concentration, the spheres start to overlap. The first nonlinearity point in the THz excess absorption graph represents the concentration at which the spheres begin to overlap.

Uniform nonoverlapping spheres can be arranged in various ways, see two examples in Figure 3a,b. The efficiency of sphere packing is expressed with a packing density coefficient $\eta = V_S/V_{UC}$, where V_S is the volume occupied by spheres in the lattice unit cell with volume V_{UC}. For nonoverlapping spheres η can range from 0.0555 for the loosest packing possible until 0.74 for close-packed face-centered cubic lattice Figure 3b. Randomly arranged spheres have the global packing density of $\eta = 0.64$.[25] However, locally any spatial arrangement has probability to occur. Therefore, the first sphere configuration at which overlapping takes place is the loosest packing possible with η = 0.0555.

The THz *excess absorption extremum* (EAE) signifies the last overlap point of the hydration shells. Further alcohol concentration increase is viewed as a unit cell shrinkage, where the spheres with a constant radius representing solute molecules with their hydration shells remain on the cube vertices. The packing density coefficient η changes with solute concentration x_A. The spheres continue overlapping until all the bulk water is consumed. The result where the last bulk water domains are consumed in partially overlapped hydration shells is shown in Figure 3c,d for simple and face-centered cubic cells. This is the case for the most frequently occurring sphere configuration at EAE. η = 2.72 (Figure 3c) is chosen for hydration shell size extraction at EAE.

The concentration at EAE reflects the transition point from a liquid phase mainly dominated by water to a liquid phase dominated by the alcohol network. We term this point at THz excess absorption extremum coefficient concentration, the *pansyllephtic point* (see Figure 2). At this point, there is no conceptual and measurable difference between solvent and solute molecules throughout the whole solution. All molecules are either part of an hydration or of an alcohol shell, and the mix is thus highly ordered like a pseudocrystal. This is what our Greek terminology defines.

Estimation of the deviation from linear behavior of the THz excess absorption in function of alcohol concentration at IAD is shown in Figure 4. Insufficient number of measurement points and some added noise make the deviation point estimation without interpolation function error-prone, if not impossible. The first six measurement points (Figure 4) lie on the interpolation function tangent line at x_A = 0 [mol/mol]. Seventh point at x_A = 0.12 [mol/mol] clearly lies outside the infinite dilution range, but the transition point is not obvious. Therefore, the infinite dilution transition point is defined by the concentration where 5% relative error exists between the linear and the interpolation functions. In the case where we make use of EAE value, the interpolation function is used as well. The minimum of the interpolation function is taken as the minimum of the THz excess absorption coefficient.

dx.doi.org/10.1021/jp305356d | J. Phys. Chem. B 2012, 116, 14071–14077

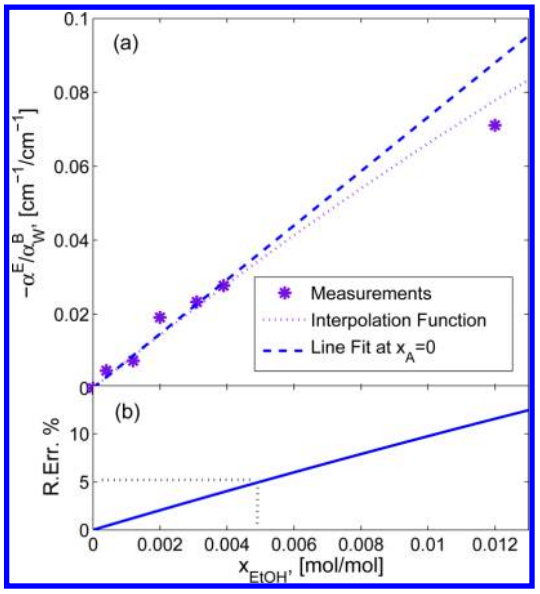

Figure 4. Procedure to estimate the THz excess absorption deviation from linear behavior for ethanol at infinite alcohol dilution: (a) absorption measurements, interpolation function and linear fit $x_A = 0$ [mol/mol]; (b) relative error of linear fit and interpolation functions.

The hydration shell size is estimated knowing the packing density coefficient η at a specific concentration x_A with the following equation:

$$N_H = \frac{\bar{V}_A(x_A)}{\bar{V}_W(x_A)}\left(\frac{\eta}{\Phi_A(x_A)} - 1\right) \tag{10}$$

where η is packing density, Φ_A alcohol volume fraction at solute molar fraction x_A. $\bar{V}_A$ and $\bar{V}_W$ are alcohol and water partial molar volumes at concentration x_A.

The hydration number N_H of lower alcohols extracted at IAD, at EAE and figures found in literature are summarized in Table 2. There is a clear trend of solute hydration shell size

Table 2. Hydration Shell Size, N_H, Extraction Results at IAD with η = 0.055, at EAE with η = 2.72 and data Found in References

	IAD		EAE		
alcohol	x_A, 5%	N_H	x_A	N_H	reference N_H
methanol	7.45×10^{-3}	5.43	0.210	13.97	16.9,[26] 15[27]
ethanol	4.90×10^{-3}	8.49	0.134	22.94	21.3,[26] 21[28]
1-propanol	4.90×10^{-3}	8.08	0.147	22.99	24.8[26]
2-propanol	3.95×10^{-3}	10.28	0.102	31.10	—
1-butanol	1.02×10^{-3}	49.86	—	—	28.4[26]

increase with the number of carbon atoms in alcohol, i.e. with the increase of hydrophobic surface area. Hydration shell numbers extracted at IAD, result in underestimations with respect to literature results. Hydration shell size extraction results at EAE are much closer to literature reference results.

Hydration Shell Absorption Coefficient Extraction. The hydration shell absorption coefficient, α_W^H, is estimated knowing N_H. In order to extract α_W^H from eq 8 containing two unknowns $\Delta\alpha_W^{HB}$ and $\Delta\alpha_A^{SB}$, a system of two equations is created. Therefore, the known mixture properties at IAD and EAE are used. At IAD: 1) all alcohol molecules are solvated, $\Phi_A = \Phi_A^S$; 2) the total hydration shell volume fraction increases linearly with the alcohol concentration, $\Phi_W^H = (\bar{V}_W/\bar{V}_A)N_H\Phi_A$. At EAE: (1) all alcohol molecules are still solvated, $\Phi_A = \Phi_A^S$; (2) all water molecules are hydrated, $\Phi_W = \Phi_W^H$. Then, the two-equation system is written as follows:

$$\begin{cases} \alpha^E(x_A^{IAD}) = \left(\Delta\alpha_W^{HB}\dfrac{\bar{V}_W(x_A^{IAD})}{\bar{V}_A(x_A^{IAD})}N_H + \Delta\alpha_A^{SB}\right)\Phi_A(x_A^{IAD}) \\ \alpha^E(x_A^{EAE}) = \Delta\alpha_W^{HB}\Phi_W(x_A^{EAE}) + \Delta\alpha_A^{SB}\Phi_A(x_A^{EAE}) \end{cases} \tag{11}$$

Estimated values of the normalized hydration shell absorption coefficient at f = 0.28 [THz] are shown in Table 3. The normalized absorption coefficient of lower aqueous alcohol hydration shell is $\alpha_W^H/\alpha_W^B = 0.774 \pm 0.028$ [cm^{-1}/cm^{-1}].

Table 3. Hydration Shell Water α_W^H and Solvation Shell Alcohol α_A^S THz Absorption Coefficients of Aqueous Alcohols at f = 0.28 [THz]

aq. alcohol	methanol	ethanol	1-propanol	2-propanol	1-butanol
α_W^H/α_W^B	0.769	0.743	0.811	0.772	—
α_A^S/α_W^B	0.694	0.612	0.730	0.587	—
α_A^S/α_A^B	3.3	5.8	12.0	11.2	—

DISCUSSIONS

The THz absorption coefficient measurements for aqueous alcohol solutions of methanol, ethanol, 1,2-propanol and 1-butanol are performed at f = 0.28 [THz] with a highly sensitive and accurate measurement technique. First the relaxation processes contributing to the absorption at this frequency are discussed. Then hydration shell packing, size, partial hydration/solvation shell absorptions are discussed. Self-association and other possible method limitations are discussed. At last the methodology improvements are suggested.

The THz excess absorption coefficient measured at f = 0.28 [THz] reflects the intermolecular interactions. At this frequency, all three Debye relaxation processes observed in aqueous alcohol solutions[19,29] are included. While the relaxation measurements up to f = 0.1 [THz][30] poorly cover the fastest relaxation process and even intermediate process at low alcohol concentrations. The dipole relaxation processes are attributed to various molecular movements, which are constrained by intermolecular interactions i.e. viscosity in accordance to the Stoke–Einstein–Debye theory. Some correlation is found between relaxation processes and liquid viscosity.[31] Excess Gibbs energy, derived from the first relaxation time constant, exhibits similar molar fraction dependency like the measured THz excess absorption.[30] The excess Gibbs energy maxima of the first relaxation time are fount at 0.30, 0.18, 0.14, and 0.15 molar fractions of aqueous methanol, ethanol, 1-propanol and 2-propanol, respectively. The positive excess Gibbs energy is caused by the stronger intermolecular interaction and therefore might explain well the negative THz excess absorption. The discrepancies can be caused by intermediate and fast relaxation processes. The relaxation process analyses in[29−31] deal with integral liquid response in terms of relaxation time-constant and strength, without dissecting a relative contribution of hydration/solvation shells. The authors strongly believe that none of the Debye relaxation processes for water–alcohol solution can be

dx.doi.org/10.1021/jp305356d | J. Phys. Chem. B 2012, 116, 14071−14077

solely attributed to specific domain (bulk or interfacial) of water or alcohol molecules.

The critical step in THz excess absorption analysis is the hydration shell packing density determination. The packing density coefficient, representing the hydration shell overlap, depends on the solute-to-solute distance (here, the distance from one solute molecule to another closest solute molecule). Let us assume that the solute-to-solute distance at any given concentration has a continuous Gaussian distribution of a probability density function. As the solute concentration increases, at IAD, the hydration shell overlap occurs gradually, first for closer molecules and then for more distant. Therefore, no sharp transition point of excess absorption is observed at IAD (see Figure 4). Obviously, the packing density coefficient is underestimated at IAD, resulting in a smaller hydration shell size. Nevertheless, the hydration shell values are on the same order of magnitude and follow similar trends with the ones found in literature (see Table 3). At EAE almost all water molecules belong to hydration shell water and all alcohol molecules are in solvation state (assuming no self-association). In this case, the hydration shell size average value is determined by a representative packing density coefficient (see Figure 3d) with the highest occurrence probability of solute-to-solute distance. Therefore, hydration shell size estimation is more accurate at the EAE.

The hydration shell size is evaluated at two concentrations considering the hydration shell packing density: (i) infinite alcohol dilution and (ii) THz excess absorption extremum, i.e., the pansyllephtic point. The hydration shell sizes, estimated at THz excess absorption extremum, are in good agreement with the data found in literature. The hydration shell size extraction proved to be more accurate at the THz excess absorption extremum than at infinite alcohol dilution. The hydration shell size extraction using the THz excess absorption extremum is a novel and more precise hydration shell size extraction technique. THz excess absorption extremum is also a transition point between water- and alcohol-dominated liquids. Hydration shell size is increasing with the size of alkane group in the alcohol molecule.

The hydration/solvation layer absorption decrease/increase relative to its bulk shows molecule dynamics alternations. The total absorption of the aqueous alcohols decreases with alcohol concentration at $f = 0.28$ [THz] partially due to substitution of slower (heavier) dipoles (ideal mixing absorption). Therefore, it is reasonable to assume that additional absorption decreases (negative excess absorption) is caused by partial water dipole dynamics retardation. The observed picosecond time-scale retardation of hydration shell by hydrophobic solutes is in agreement with molecular dynamics simulations[10] and infrared spectroscopy[9] results. Hydration water absorption has marginal variation with alcohol alkane group size. The normalized absorption coefficient of lower aqueous alcohol hydration shell is $\alpha_W^H/\alpha_W^B = 0.774 \pm 0.028$ [cm^{-1}/cm^{-1}]. The dynamics retardation is caused by the predominantly hydrophobic exposed surfaces in the alcohol molecule. Trehalose, lactose and glucose have higher hydration shell water absorption than bulk water absorption.[32] This can be attributed to a higher density of hydrophilic groups in the molecule resulting in the hydration shell water molecule dynamics acceleration. The solvation shell alcohol molecules absorb more than the bulk alcohol molecules, $\alpha_A^S > \alpha_A^B$. Additionally, the ratio of solvated to bulk alcohol absorption α_A^S/α_A^B increases with the alcohol size. At high concentration, alcohol molecules tend to form polymeric chain structures. Added water molecules increase the chain segmentation. The chain-end alcohol molecules have lower binding, therefore they are less restrained to the movement and exhibit stronger absorption. This complies with the[29] findings, where the increase in the absorption is shown for the relaxation process of the third order Debye model attributed to the alcohol chain-ends. The influence of water on the alcohol structure is more pronounced for the larger alcohols.[30]

When alcohol molecules overcome a certain concentration threshold they tend to self-associate and cluster. Interior molecules in the cluster exhibit bulk like properties and the amount of hydrated water is reduced. Hydration shell size extraction at THz excess absorption extremum is valid under the condition that no solute self-association occurs at the concentrations of interest. In low-alcohol concentration solutions, alcohol molecules exist as monomers with hydration shells around them, at higher alcohol concentrations when bulk water is consumed in the hydration shells they begin to form micelles.[33] Excess absorption graph concavity ($\partial^2\alpha^E/\partial x_A^2 < 0$), i.e. mixture absorption exhibits higher rate of change toward bulk-like properties in function of alcohol concentration, might indicate alcohol self-association. Minimum alcohol concentrations, where $\partial^2\alpha^E/\partial x_A^2 < 0$ are 0.31, 0,33, 0.20 for ethanol, 1-propanol and 2-propanol, respectively. Mixtures with alcohol concentrations higher than in azeotropic composition (x_{az} = 0.89, 0.44 [mol/mol] for Ethanol and 1-Propanol) have higher alcohol−alcohol than water−alcohol interaction energy,[34] leading to self-associated alcohol clusters. Methanol molecule clustering in aqueous mixtures has been experimentally observed by proton diffraction measurements and theoretically by molecular dynamics simulation for $x_A > 0.27$ [mol/mol][35] which is above the THz excess absorption extremum. 1-propanol excess absorption fitting with interpolation function in eq 9 results in a noticeably higher standard error, meaning that the shape could not be resembled well with the three components of the fitting function. A possible explanation is the higher tendency of 1-propanol to self-associate at lower concentrations. Fourier transform infrared spectroscopy of aqueous 1-propanol reveals an increased number of 1-propanol with gauche conformation, indicating a polymerization of 1-propanol alcohol, starting from $x_A > 0.05$ [mol/mol].[36]

The hydration/solvation shell parameters obtained within the proposed methodology are absorption step-function equivalents. A stepwise approximation (assumptions 1, 2, and 6) is used for quasi-continuously varying function of absorption in the interfacial layer. In the hydration shell, water absorption coefficient gradually increases along the consecutive hydration layers (or water molecule dynamics retardation decreases) with the distance from its alcohol molecule until the absorption becomes equal to bulk water absorption at the edge of hydration shell. Because of the hydration shell overlapping, which starts from the more absorbing outer layers of hydration shell, the average absorption per single hydration shell is reduced with the alcohol concentration increase. This slow-water relaxation time in TMU−water solution is shown to increase at high solute concentrations,[31] signifying the absorption reduction of hydration shell water. This may lead to inaccuracies in absorption derivation at EAE and bias the results, depending on the shape of the hydration water absorption profile versus distance. At $f = 0.28$ [THz] the hydrated water absorption reduction by a factor of 0.774, relative to bulk water, translates to the relaxation time constant

(for both slow and fast relaxation processes[29]) increase by a factor of 1.41 (the relaxation strengths are unchanged). This dynamics retardation factor found to be in a good agreement with,[37] where using MD simulations it is shown that a comparable solvent TMAO introduces the reorientation retardation factor of 1.5.

The impact of other less critical assumptions is considered here: (4) Inaccuracy introduced for small alcohol molecules is negligible, however the shape might be important for larger molecules. (7) Hydration and solvation shell densities are different from bulk. Nevertheless the derivation at THz excess extremum absorption is marginally affected since almost all material present at this composition is hydration or solvation shell.

The proposed hydration shell property determination at THz excess absorption extremum based on geometrical hydration shell packing consideration is a good first level model. However, more accurate hydration shell packing density determination is needed, especially for solutes which defy the assumptions. Moreover, with the packing density versus solute concentration dependency, one would be able to fit the data over the entire composition range. To this end, Monte Carlo method is applicable to determine average packing density for a multitude of concentrations. Nevertheless the concentration dependent packing density coefficient should include self-association, molecule geometry and hydrophilic/hydrophobic surface distribution effects.

SUMMARY AND CONCLUSIONS

The developed methodology, demonstrated for lower monohydric alcohols, allows to directly determine solute molecules hydration shell parameters from the THz absorption coefficient measurements within a certain set of concentrations. The THz excess absorption extremum or pansyllephtic point is a significant point, at this concentration there are no bulk like domains. The hydration shells of alcohols are 13.97, 22.94, 22.99, 31.10 for methanol, ethanol, 1- and 2-propanols, respectively. The hydration shell water THz absorption coefficients at f = 0.28 [THz] for these alcohols is α_W^H/α_W^B = 0.774 ± 0.028[cm^{-1}/cm^{-1}]. The solvation shell alcohol THz absorption coefficients at f = 0.28 [THz] are 0.694, 0.612, 0.730, 0.587 for methanol, ethanol, 1- and 2-propanols, respectively. An implication of the hydration shell is the possibility to study long-range interactions between macromolecules caused by the molecules hydration shell.

AUTHOR INFORMATION

Corresponding Author

*E-mail: vmatveje@etro.vub.ac.be..

Notes

The authors declare no competing financial interest.

ACKNOWLEDGMENTS

This work has been partially funded by the Industrial Research Fund of VUB, IOF242: "ETROs innovation and valorization framework: Crossing boundaries with visionary Electronics & ICT" and IMEC BISENS laboratory. The first author is thankful to IMEC (Leuven, Belgium) for its scholarship program.

REFERENCES

(1) Grossman, M.; Born, B.; Heyden, M.; Tworowski, D.; Fields, G. B.; Sagi, I.; Havenith, M. *Nat. Struct. Mol. Biol.* **2011**, *18*, 1102−U113.
(2) Heyden, M.; Havenith, M. *Methods* **2010**, *52*, 74−83.
(3) Luong, T. Q.; Verma, P. K.; Mitra, R. K.; Havenith, M. *Biophys. J.* **2011**, *101*, 925−933.
(4) Sterpone, F.; Stirnemann, G.; Hynes, J. T.; Laage, D. *J. Phys. Chem. B* **2010**, *114*, 2083−2089.
(5) Rezus, Y. L. A.; Bakker, H. J. *Phys. Rev. Lett.* **2007**, *99*, 148301.
(6) Falconer, R.; Markelz, A. *J. Infrared Millim. Terahertz Waves* **2012**, 1−16.
(7) Tonouchi, M. *Nat. Photonics* **2007**, *1*, 97−105.
(8) Heugen, U.; Schwaab, G.; Bruendermann, E.; Heyden, M.; Yu, X.; Leitner, D. M.; Havenith, M. *Proc. Natl. Acad. Sci. U.S.A.* **2006**, *103*, 12301−12306.
(9) Bakulin, A. A.; Pshenichnikov, M. S.; Bakker, H. J.; Petersen, C. *J. Phys. Chem. A* **2011**, *115*, 1821−1829.
(10) Stirnemann, G.; Castrillon, S. R.-V.; Hynes, J. T.; Rossky, P. J.; Debenedetti, P. G.; Laage, D. *Phys. Chem. Chem. Phys.* **2011**, *13*, 19911−19917.
(11) Nandi, N.; Bhattacharyya, K.; Bagchi, B. *Chem. Rev.* **2000**, *100*, 2013−2045.
(12) Fidler, J.; Rodger, P. *J. Phys. Chem. B* **1999**, *103*, 7695−7703.
(13) Leitner, D. M.; Gruebele, M.; Havenith, M. *HFSP J* **2008**, *2*, 314−323.
(14) Born, B.; Havenith, M. *J. Infrared Millim. Terahertz Waves* **2009**, *30*, 1245−1254.
(15) Niehues, G.; Heyden, M.; Schmidt, D. A.; Havenith, M. *Faraday Discuss.* **2011**, *150*, 193−207.
(16) Matvejev, V.; de Tandt, C.; Ranson, W.; Stiens, J.; Vounckx, R.; Mangelings, D. *Prog. Electromagn. Res.* **2011**, *121*, 89−101.
(17) Matvejev, V.; De Tandt, C.; Ranson, W.; Stiens, J. *Wet silicon bulk micromachined THz waveguides for low-loss integrated sensor applications*. 35th International Conference on Infrared, Millimeter, and Terahertz, Rome, Italy, September 5−10, 2010.
(18) Nagel, M.; Foerst, M.; Kurz, H. *J. Phys.-Condes. Matter* **2006**, *18*, S601−S618.
(19) Yomogida, Y.; Sato, Y.; Nozaki, R.; Mishina, T.; Nakahara, J. *J. Mol. Struct.* **2010**, *981*, 173−178.
(20) Vij, J.; Simpson, D.; Panarina, O. *J. Mol. Liq.* **2004**, *112*, 125−135.
(21) Pozar, D. *Microwave Engineering*; Wiley: New York, 2004.
(22) Ref 21, p 29.
(23) Zarei, H. A.; Jalili, F.; Assadi, S. *J. Chem. Eng. Data* **2007**, *52*, 2517−2526.
(24) Dethlefsen, C.; Sorensen, P.; Hvidt, A. *J. Solution Chem.* **1984**, *13*, 191−202.
(25) Jaeger, H.; Nagel, S. *Science* **1992**, *255*, 1523−1531.
(26) Graziano, G. *Phys. Chem. Chem. Phys.* **1999**, *1*, 3567−3576.
(27) van Erp, T.; Meijer, E. *Chem. Phys. Lett.* **2001**, *333*, 290−296.
(28) van Erp, T.; Meijer, E. *J. Chem. Phys.* **2003**, *118*, 8831−8840.
(29) Moller, U.; Cooke, D. G.; Tanaka, K.; Jepsen, P. U. *J. Opt. Soc. Am. B-Opt. Phys* **2009**, *26*, A113−A125.
(30) Sato, T.; Buchner, R. EuroConference on Molecular Liquids - Routes from Local Order to Large Scale Cooperativity, Castelvecchio Pascoli, Italy, Sep 05−10, 2003*J. Mol. Liq.* **2005**, *117*, 23−31.
(31) Tielrooij, K.-J.; Hunger, J.; Buchner, R.; Bonn, M.; Bakker, H. J. *J. Am. Chem. Soc.* **2010**, *132*, 15671−15678.
(32) Heyden, M.; Bruendermann, E.; Heugen, U.; Niehues, G.; Leitner, D. M.; Havenith, M. *J. Am. Chem. Soc.* **2008**, *130*, 5773−5779.
(33) Onori, G.; Santucci, A. *J. Mol. Liq.* **1996**, *69*, 161−181.
(34) Wakisaka, A.; Matsuura, K.; Uranaga, M.; Sekimoto, T.; Takahashi, M. *J. Mol. Liq.* **2011**, *160*, 103−108.
(35) Dougan, L.; Bates, S.; Hargreaves, R.; Fox, J.; Crain, J.; Finney, J.; Reat, V.; Soper, A. *J. Chem. Phys.* **2004**, *121*, 6456−6462.
(36) Tong, H.-J.; Yu, J.-Y.; Zhang, Y.-H.; Reid, J. P. *J. Phys. Chem. A* **2010**, *114*, 6795−6802.
(37) Laage, D.; Stirnemann, G.; Hynes, J. T. *J. Phys. Chem. B* **2009**, *113*, 2428−2435.